MDPI

Article

Effect of Q235 Hot-Dip Galvanized and Post-Casting T6 Heat Treatment on Microstructure and Mechanical Properties of Interfacial between AZ63 and Q235 by Solid-Liquid Compound Casting

Jiahong Dai [1,2,3,4]**, Hongmei Xie** [1]**, Yangyang Zhou** [1]**, Qin Zou** [2,*]**, Yuan Tian** [5]**, Qingshan Yang** [6,*]**, Cheng Peng** [1]**, Bin Jiang** [2] **and Jianyue Zhang** [7,*]

[1] College of Materials Science and Engineering, Yangtze Normal University, Chongqing 408102, China; daijiahong@yznu.edu.cn (J.D.); xiehongmei@yznu.edu.cn (H.X.); 202024591237@stu.yznu.edu.cn (Y.Z.); 20090008@yzun.edu.cn (C.P.)

[2] National Engineering Research Center for Magnesium Alloys, College of Materials Science and Engineering, Chongqing University, Chongqing 400044, China; jiangbinrong@cqu.edu.cn

[3] Chongqing Jiulongyuan High-Tech Industry Group Co., Ltd., Chongqing 400080, China

[4] Loncin Industry Co., Ltd., Chongqing 400080, China

[5] Chongqing Materials Research Institute Co., Ltd., Chongqing 400707, China; tianyuan@cmri.cc

[6] School of Metallurgy and Material Engineering, Chongqing University of Science and Technology, Chongqing 401331, China

[7] Department of Materials Science and Engineering, The Ohio State University, Columbus, OH 43210, USA

* Correspondence: zouqin17@cqu.edu.cn (Q.Z.); qsyang@cqu.edu.cn (Q.Y.); zhang.12278@osu.edu (J.Z.)

Abstract: AZ63 sacrificial anode is widely used to protect buried metal pipelines and reinforced concrete structures and so on. The interfacial metallurgical bonding between AZ63 sacrificial anode and Q235 wiring terminal directly affects its cathodic protection performance. Therefore, microstructure and mechanical properties of interfacial between AZ63 and Q235 by solid–liquid compound casting with hot-dip galvanized and post-casting solution-aging treatment (T6) were investigated. The results indicate that hot-dip galvanizing on the surface of Q235 is beneficial to the formation of intermetallic compounds at the interface. At the same time, it can promote the metallurgical bonding of the interface between AZ63 and Q235. After T6 heat treatment, the intermetallic compound at the interface between AZ63 and galvanized Q235 was refined. The electron-probe microanalyzer (EPMA) revealed that the intermetallic compounds at the interfaces between AZ63 and galvanized Q235 were Fe_2Al_5 before and after T6 treatment. Push-out testing and microhardness were used to investigate the mechanical properties of interface between AZ63 and Q235. It is shown that the hot-dip galvanization of the Q235 surface and T6 treatment were beneficial to improve the metallurgical bonding shear strength and microhardness of the interface. After T6 heat treatment, the highest shear strength at the interface between AZ63 and galvanized Q235 was up to 31.9 ± 1.9 MPa.

Keywords: AZ63; galvanized; T6 heat treatment; solid–liquid compound casting

1. Introduction

Magnesium (Mg) sacrificial anodes are widely used to protect buried metal pipelines, reinforced concrete structures, and other steel structures, due to their inherent negative potential, large driving voltage, and large current output per unit weight [1–4]. The current commercial use of magnesium alloy sacrificial anode is mainly focused on casting AZ63, as it has uniform surface dissolution and high current efficiency [5–7]. In order to facilitate the connection between AZ63 sacrificial anode and protected pipelines or steel structure, when casting AZ63 sacrificial anode, Q235 rod is first placed in the mold, and then the solid–liquid interface is combined to form a wiring terminal. The interfacial metallurgical

bonding between AZ63 sacrificial anode and Q235 directly affects its cathodic protection performance, so the solid–liquid compound casting process is very important.

The melting point, thermal conductivity, and thermal expansion coefficient of magnesium alloys and steels are quite different [8]. Furthermore, according to the Fe–Mg phase diagram, the solubility of Fe in Mg is 0.00043 at.% at 923 K, while the solid solubility of Mg in Fe is close to zero [9]. At the same time, Fe and Mg elements do not react to each other [10]. Therefore, it is difficult to form a metallurgical bonding between Mg and Fe. In recent years, there have been a number of reports on the solid–liquid composite casting of magnesium alloy and steel [11–15]. Sacerdote-Peronnet et al. reported the effects of varying the degree of chemical interaction and specimen thickness on the load–displacement curves between mild steel and magnesium base Mg–Al alloy [11]. However, the metallurgical bonding of the interface is not good, and the strength is low. The main function of galvanizing steel is to prevent the surface from being oxidized [16]. Moreover, Zinc coating on steel surface will promote the formation of low melting Mg–Zn eutectic, which can improve the weldability of AZ31 and steel [17]. Cheng et al. and Jiang et al. studied that the microstructure and mechanical properties of interfacial between AZ91D and 45 steel by solid–liquid composite casting with hot-dip galvanized and hot-dip aluminized 45 steel bars at 720 and 780 °C, respectively [12–14]. Zhao et al. [15] systematically analyzed the microstructure and mechanical properties of the bonding interface of AZ91D/Al-coated 0Cr19Ni9 bimetal materials by using liquid–solid compound casting. Galvanizing and aluminizing on the iron surface can obviously improve the metallurgical bonding and strength of the interface between iron and AZ91 magnesium alloy. However, the composite casting of AZ63 and Q235 has not been reported. Literature studies have found that solution-aging-treatment (T6) heat treatment can improve the performance of sacrificial anode of AZ63 [18]. In addition, T6 heat treatment can also promote element diffusion between AZ63 and Q235.

In the present study, Q235 steel, hot-dip galvanized Q235 steel, and AZ63 magnesium alloy were selected as the experimental materials for solid–liquid compound casting process. After casting, the composite casting samples of AZ63 magnesium alloy and galvanized steel Q235 were subjected to T6 heat treatment. The microstructural features, shear strengths, and microhardness at the interface were examined. The interface reaction mechanisms of AZ63 and Q235 were also discussed.

2. Experimental

Commercially AZ63 magnesium alloy ingots and Q235 steel core with a diameter of 10 mm were used in this study, and their chemical compositions measured by ICP–OES (AGILENT 730, Agilent Technologies Inc., California, CA, USA) are listed in Table 1. Q235 steel for hot-dip galvanized treatment at 445–450 °C was used in the experiments. The Q235 steel core was used as a control group.

Table 1. Chemical composition of AZ63 and Q235 (wt.%).

Materials	Al	Zn	Ni	Cu	Mn	Si	Mg	C	S	P	Fe
AZ63	5.7	3.1	0.001	0.002	0.51	0.08	Bal.	-	-	-	0.004
Q235	-	-	-	-	0.5	0.3	-	0.12	0.04	0.0035	Bal.

The AZ63 magnesium alloy ingots were melted by using electrical furnaces (Hefei Kejing Materials Technology Co., Ltd., Hefei, China). The protective gas atmosphere of the AZ63 magnesium alloy melt was the CO_2 + 0.5% vol. SF_6. When the temperatures of the AZ63 magnesium alloy melts reached 720 °C, the oxide scale of the molten metals was skimmed. The AZ63 magnesium alloy melt was poured into a metal die with a pre-positioned Q235 steel core. After solidification, the AZ63 magnesium alloy sacrificial anode was finally obtained. The sample obtained by composite casting is shown in Figure 1. Finally, the AZ63 magnesium alloy with a galvanized steel Q235 bar underwent T6 heat treatment at 385 °C for 10 h and aging at 220 °C for 5 h.

Figure 1. The sample obtained by composite casting.

In order to observe the interfacial microstructure, the metallographic cross-sections of the specimens were machined from the vertical direction of the Q235 steel core by the electrical discharge wire-cutting machine. Next, the specimens were grounded.

The interfacial microstructure was characterized by optical microscope (OM, NM910, Nanjing Jiangnan Novel Optics Co., Ltd., Nanjing, China) and scanning electron microscope (SEM, JEOL JSM 7100F, Joint-stock Company, Tokyo, Japan) equipped with an energy-dispersive X-ray spectroscope of Oxford X-Max EDS (Oxford Instrument Technology Co., Ltd., Oxford, UK). The elemental distributions were analyzed by using an electron-probe microanalyzer (EPMA, EPMA-1720H, Shimadzu Corporation, Kyoto, Japan).

The shear strength of the interfacial between AZ63 and Q235 was investigated by push-out testing (NEW SANSI CMT-5105, Xinsansi Enterprise Development Co., Ltd., Shanghai, China). A schematic diagram of the push-out test is shown in Figure 2. The thickness of the specimens was 8 mm. The loading rate was 0.5 mm/min. Three were used for push-out testing. The shear strength (τ) was calculated by using the following equation:

$$\tau = \frac{F}{2\pi rt} \tag{1}$$

where *F* is the maximum load, *r* is the radius of Q235 steel, and *t* is the specimen thickness.
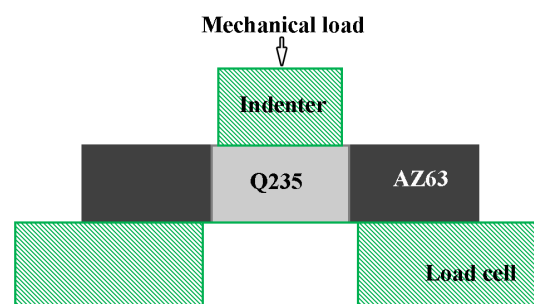

Figure 2. Schematic diagram of the push-out test.

The microhardnesses of the interface for the AZ63 and Q235 were measured by using an HV-1000 hardness tester (Shanghai Wumo Optical Instrument Co., Ltd., Shanghai, China) with a load of 100 g for 10 s. The microhardness value was evaluated by averaging the three measurements. The test was repeated three times, and the average values were reported for each sample.

3. Results and Discussion

3.1. Galvanized Q235 Microstructure

An optical micrograph of the cross-section of the galvanized Q235 is shown in Figure 3. It can be seen that the pearlite content on the surface of Q235 is obviously less than that on the core of Q235, and a decarburized layer of about 80 μm was formed on the surface of the

cross-section of the Q235 galvanized steel due to the high temperature used in the Q235 hot-dip galvanizing process.
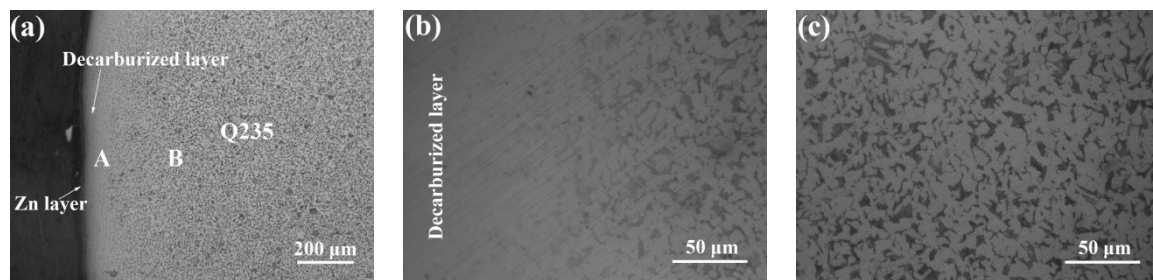

Figure 3. (**a**) Optical micrograph of the cross-section of the galvanized Q235, (**b**) magnified image of region A, and (**c**) magnified image of the region B.

A back scattered electron (BSE) micrograph of the cross-section of the galvanized Q235 is shown in Figure 4. It can be seen clearly that the Q235 surface has a more uniform thickness of zinc coating; its average thickness is about 28 μm. The EDS mapping and pointing of the zinc coating showed that the zinc coating was mainly composed of a zinc element, and no Fe–Zn intermetallic compound was formed.
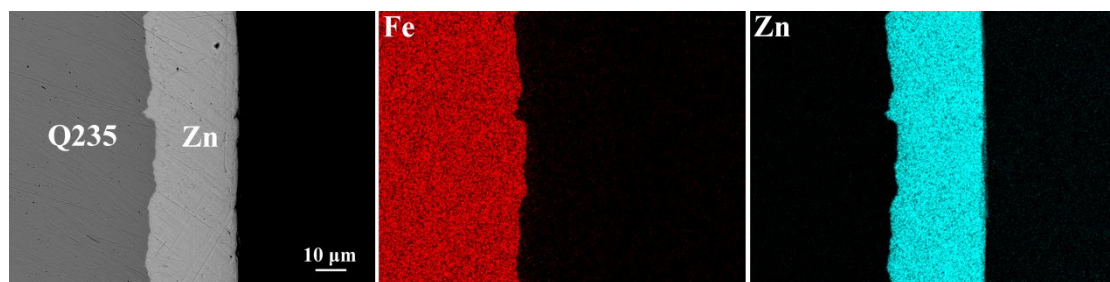

Figure 4. Mapping of the galvanized Q235.

3.2. Microstructure of the Interfaces between AZ63 and Q235 Bimetallic Composites

Optical micrographs of the interfaces between AZ63 and Q235 bimetallic composites are shown in Figure 5. It can be observed that the pearlite decreases obviously near the Q235 matrix interface and forms a decarburized layer of about 300 μm in thickness at the interface of the AZ63/Q235 and AZ63/galvanized Q235. Moreover, the thickness of the decarbonization layer is significantly wider than before casting in galvanized Q235. After T6 treatment, the decarbonization layer was about 350 μm. Both composite casting and T6 treatment can increase the thickness of the decarburization layer on Q236 surface. Therefore, high temperature promotes the formation of a decarburized layer on the surface of Q235.

Figure 6 shows the BSE micrographs of the interfaces between the AZ63 and Q235 bimetallic composites. It can clearly be seen that a small amount of intermetallic compounds is formed at the interface of AZ63/Q235, and a transition layer with an average thickness of about 15 μm is formed at the interface of AZ63/galvanized Q235. Obviously, the hot-dip-galvanized Q235 surface significantly improved the weldability of AZ63 magnesium alloy and Q235. After T6 heat treatment, the average thickness of the transition layer between the AZ63 and galvanized Q235 base layer was still about 15 μm, but the thickness of the transition layer became more uniform, and the size of the intermetallic compound was obviously refined. Meanwhile, the initial Mg–Al phase in the AZ63 matrix was dissolved by solid solution, and the dispersed fine second phase was precipitated by aging, because T6 treatment promoted the diffusion of elements at the interface, and the intermetallic compounds at the interface decreased significantly compared with those before heat treatment.
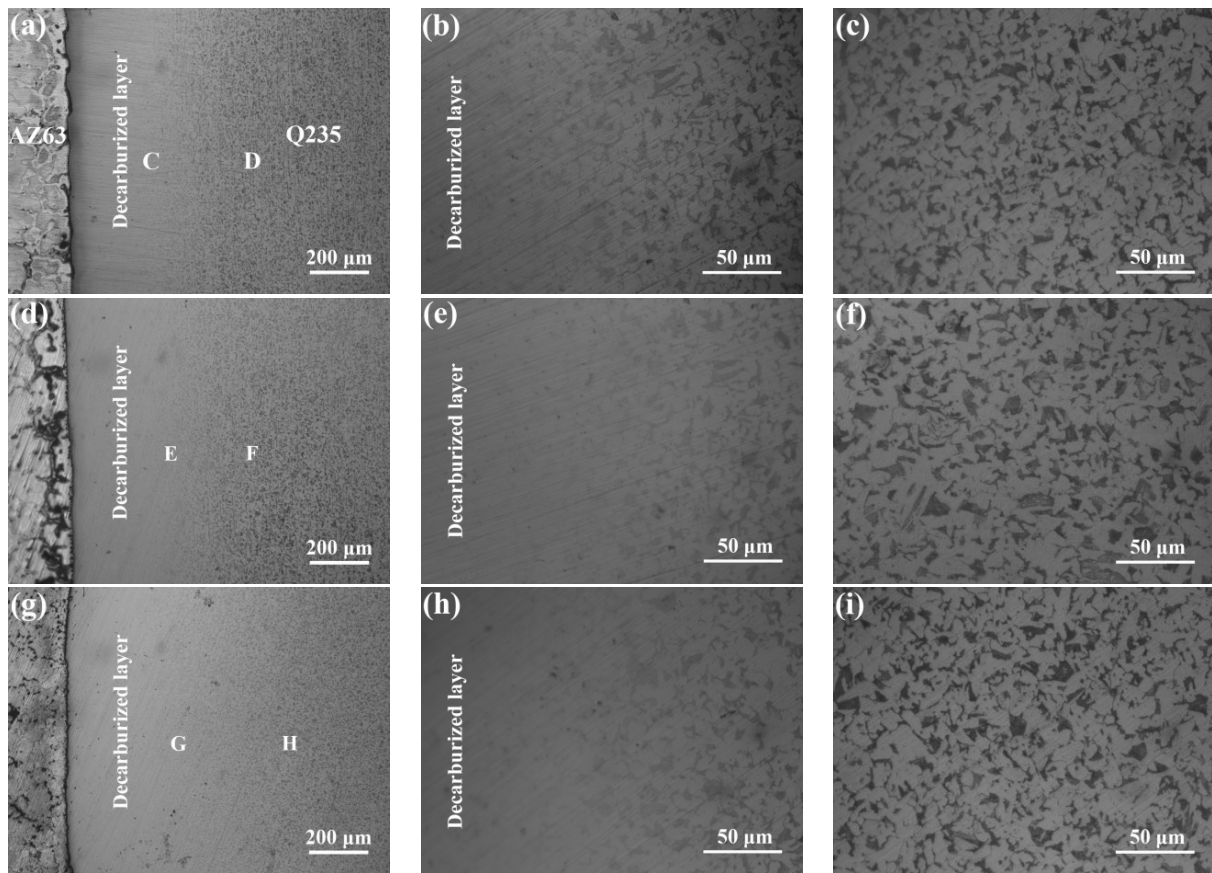
Figure 5. Optical micrographs of the interfacial of (**a**) AZ63/Q235, (**d**) AZ63/galvanized Q235, and (**g**) AZ63/galvanized Q235 + T6; (**b**) magnified image of the region C, (**c**) magnified image of the region D, (**e**) magnified image of the region E, (**f**) magnified image of the region F, (**h**) magnified image of the region G, and (**i**) magnified image of the region H.
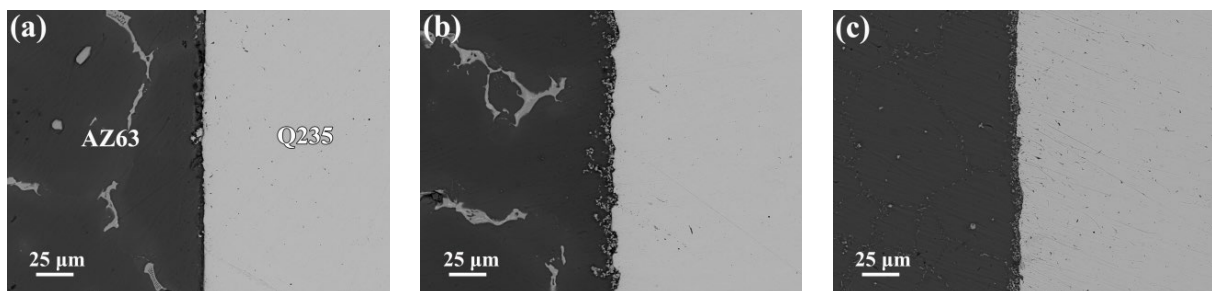

Figure 6. BSE micrographs of the interfacial of (**a**) AZ63/Q235, (**b**) AZ63/galvanized Q235, and (**c**) AZ63/galvanized Q235 + T6.

Figure 7 shows the elements distribution for the interfacial of AZ63 and Q235. It is observed that there is no obvious diffusion of Al, Mn, and Fe elements at the interfaces of AZ63/Q235. Compared with the distribution of the elements at the interface of AZ63/Q235, the Al, Mn and Fe elements are obviously aggregated at the interface of AZ63/galvanized Q235. However, the zinc on the surface of galvanized Q235 melts into AZ63 magnesium alloy during casting. After T6 treatment, the Al, Mn, and Zn elements in the matrixes were uniformly distributed, but the Al element at the interface was obviously increased, while the Mn element was obviously decreased.
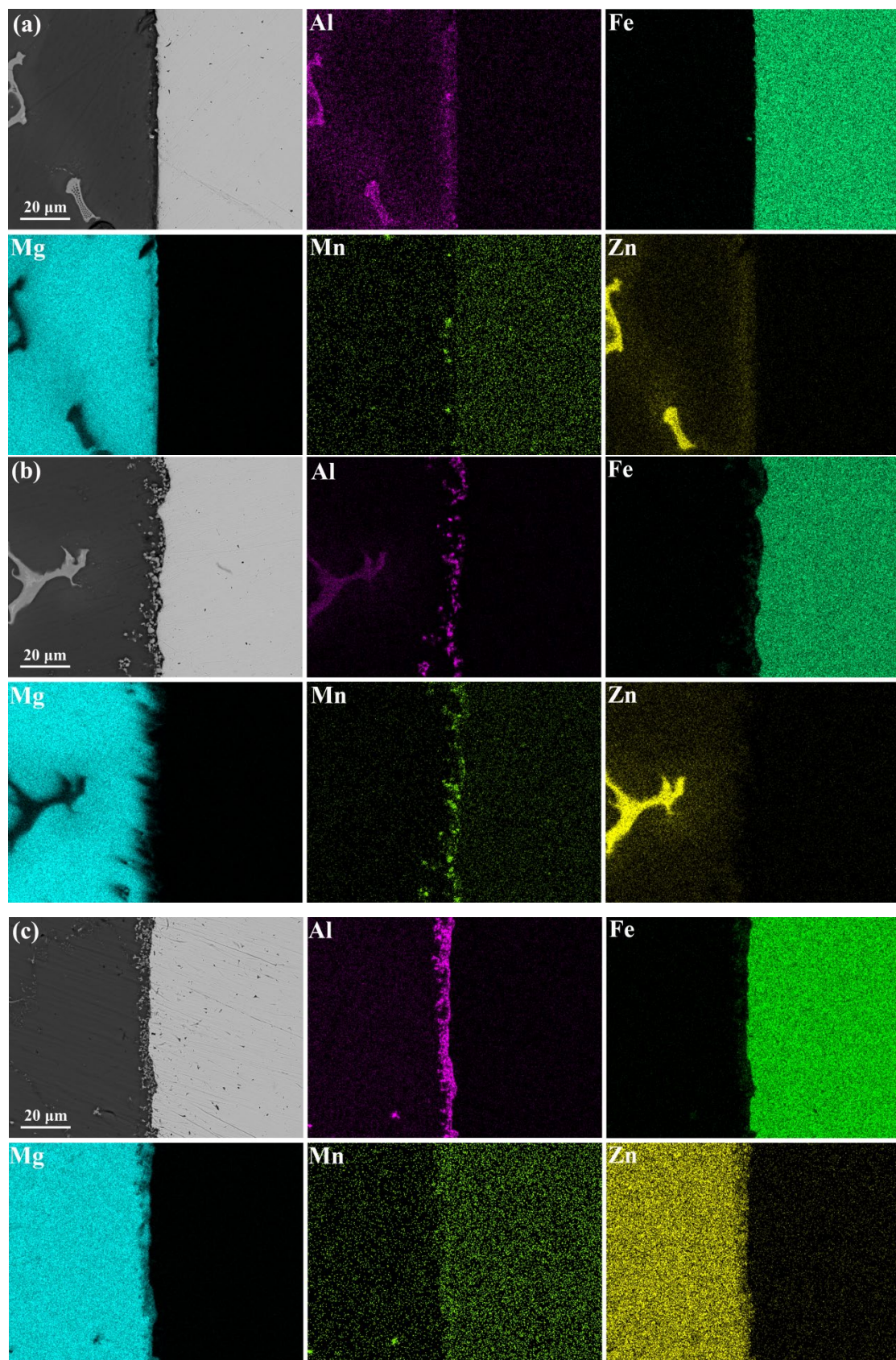
Figure 7. EDS mapping of the interfacial of (**a**) AZ63/Q235, (**b**) AZ63/galvanized Q235, and (**c**) AZ63/galvanized Q235 + T6.

According to the Fe–Mg phase diagram [9], there is no intermetallic compound between Fe and Mg, and the solid solution of Fe in the magnesium melt is very low, which may cause the interfacial reaction between Q235 steel and AZ63 magnesium alloy melt to be difficult. However, Zn can react with Fe and Mg to form metal compounds, and Zn has a higher solid solubility in Fe and Mg, so the metallurgical bonding between AZ63 and Q235 can be promoted by zinc plating on the surface of Q235, and the further diffusion of elements at the interface can be promoted by T6 treatment.

The values of the heat of formation of the major binary metal systems at the AZ63/Q235 interface are found by consulting the literature, and they are shown in Table 2 [19]. It can be seen that the heat used for the formation of Al–Mn and Al–Fe systems is relatively the lowest, so the Al–Mn and Al–Fe compounds are easily formed at the interface, and this promotes the enrichment of Al, Mn, and Fe elements at the interface.

Table 2. The values of the heat of formation (ΔH_{AB}^{mix}) for the major binary metal systems in this study.

A–B	Al–Fe	Al–Mg	Al–Mn	Al–Zn	Fe–Mn	Fe–Zn	Mg–Mn	Mg–Zn	Mn–Zn
ΔH_{AB}^{mix} (kJ/mol)	−11	−2	−10	1	0	4	10	−4	−6

To further investigate the phase composition of the interface, the BSE micrographs of the interfacial magnification of AZ63/galvanized Q235 and AZ63/galvanized Q235 + T6 are shown in Figure 8. It is observed that the intermetallic compound at the interface of AZ63/galvanized Q235 was refined after the T6 treatment. The EPMA results of the intermetallic compound at the interface are shown in Table 3. According to the Fe/Al value, the intermetallic compound at the interfaces of AZ63/galvanized Q235 is Fe_2Al_5 before and after T6 treatment.
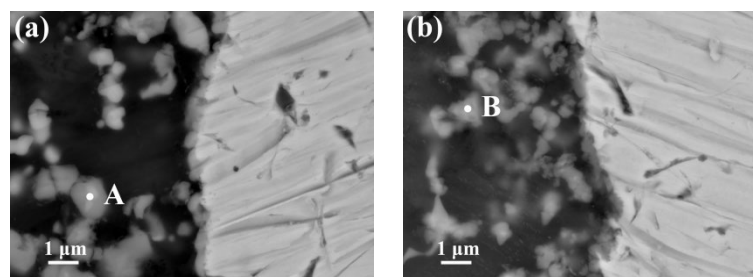

Figure 8. BSE micrographs of the interfacial magnification of (**a**) AZ63/galvanized Q235 and (**b**) AZ63/galvanized Q235 + T6.

Table 3. EPMA results taken from points A and B in Figure 8 (at.%).

Point	C	Fe	Al	Mn	Mg	Zn	Fe/Al
A	4.417	20.374	48.802	16.821	9.439	0.146	0.41
B	6.347	16.66	41.766	3.961	30.633	0.633	0.40

According to the Al–Fe phase diagram [20], intermetallic compounds of Fe_3Al, FeAl, $FeAl_2$, $FeAl_3$, and Fe_2Al_5 can be formed in Al–Fe system. However, according to Gibbs free energy change during the formation of intermetallic compound [21], the Fe_2Al_5 phase is formed earlier than the other Al–Fe intermetallic phases because the Gibbs free energy of Fe_2Al_5 intermetallics is the smallest at this experimental temperature.

3.3. Reaction Mechanism of AZ63 and Q235 Interfaces

The metallurgical reaction mechanism of AZ63/galvanized Q235 interface during solid–liquid casting and T6 treatment was clarified with the schematic diagram shown in Figure 9. In the process of solid–liquid composite casting, the melt temperature of AZ63

magnesium alloy is 720 °C, which is much higher than the melting point of zinc, so the zinc layer on the surface of Q235 will be melted quickly and enter into the melt of AZ63 magnesium alloy. The Al and Mn elements in the AZ63 magnesium alloy melt and diffuse to the interface and form $(Fe, Mn)_2Al_5$ intermetallic compound, because Mn has a similar atomic structure to Fe, and Mn substitutes for Fe in the Fe_2Al_5 phase. At the same time, the carbon element in the Q235 matrix diffuses to the surface to form a decarburized layer. During the T6 heat treatment of the AZ63/galvanized Q235 samples, the Al element in the AZ63 matrix diffused to the interface, the Mn element at the interface diffused into the Q235 matrix, and the carbon element in the Q235 matrix continued to diffuse to the interface. The size of the Fe_2Al_5 intermetallic compound at the interface is significantly smaller than that before the T6 heat treatment, and the thickness of the decarburized layer in the Q235 matrix becomes larger.
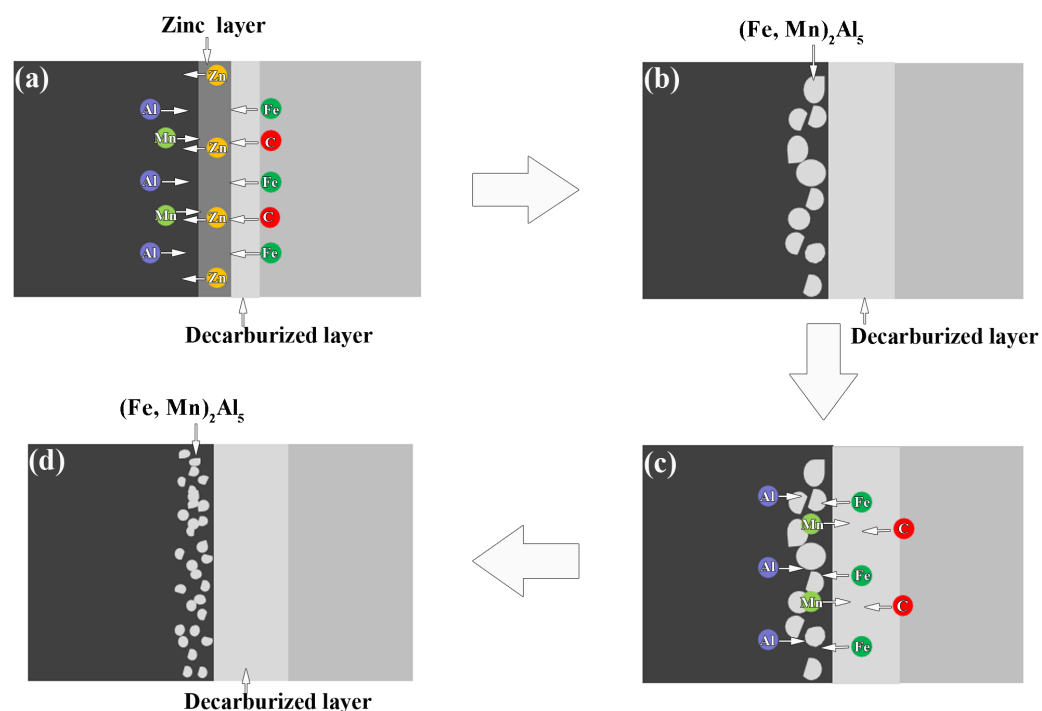

Figure 9. Schematic illustrations of reaction mechanism for AZ63 and Q235 interfaces. (**a**) The casting cooling process, (**b**) After cooling, (**c**) T6 heat treatment process, and (**d**) After T6 heat treatment.

3.4. Mechanical Properties

Figure 10 shows the load–displacement curves. It can be seen that the shear strength of AZ63/Q235, AZ63/galvanized Q235, and AZ63/galvanized Q235 + T6 metallurgical bonding presents an increasing tendency. The reason is that the surface of Q235 steel was treated by hot-dip galvanization, which promoted the metallurgical bonding of the interface, and then the T6 treatment promoted the diffusion of the interface elements, which made the metallurgical bonding of the interface closer, thus increasing the shear strength of the interface. The average shear stress at the interface can be evaluated by using Equation (1). The results are shown in Table 4. The shear strengths of AZ63/galvanized Q235 interface before and after T6 treatment in this experiment are higher than that Cheng et al. [13] evaluated the shear strength of the AZ91D/galvanized Q235 interface to be before and after heat treatment with 250 °C for 3 h.

Figure 11 shows SEM fractographs on the Q235 side of the AZ63/Q235, AZ63/galvanized Q235, and AZ63/galvanized Q235 + T6 metallurgical bonding push-out samples. The EDS results taken from points C, D, and E are shown in Table 5. It shows that the fracture surface of the Q235 side adhesion is AZ63 magnesium alloy. Moreover, it can be seen that there is less AZ63 magnesium alloy adhered to the fracture surface of the Q235 side of

the AZ63/Q235 specimen compared to the AZ63/galvanized Q235, and the machining traces on the surface of Q235 before solid–liquid composite casting can be clearly seen. However, a large amount of AZ36 magnesium alloy was obviously adhered to the surface of the Q235 side of the AZ63/galvanized Q235 and AZ63/galvanized Q235 samples after the T6 treatment shear test. It shows that the interface bonding of AZ63/galvanized Q235 and AZ63/galvanized Q235 samples treated by T6 is obviously better than that of the AZ63/Q235 interface.
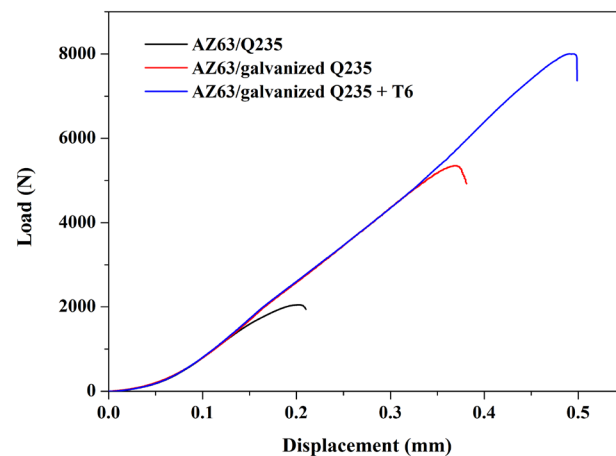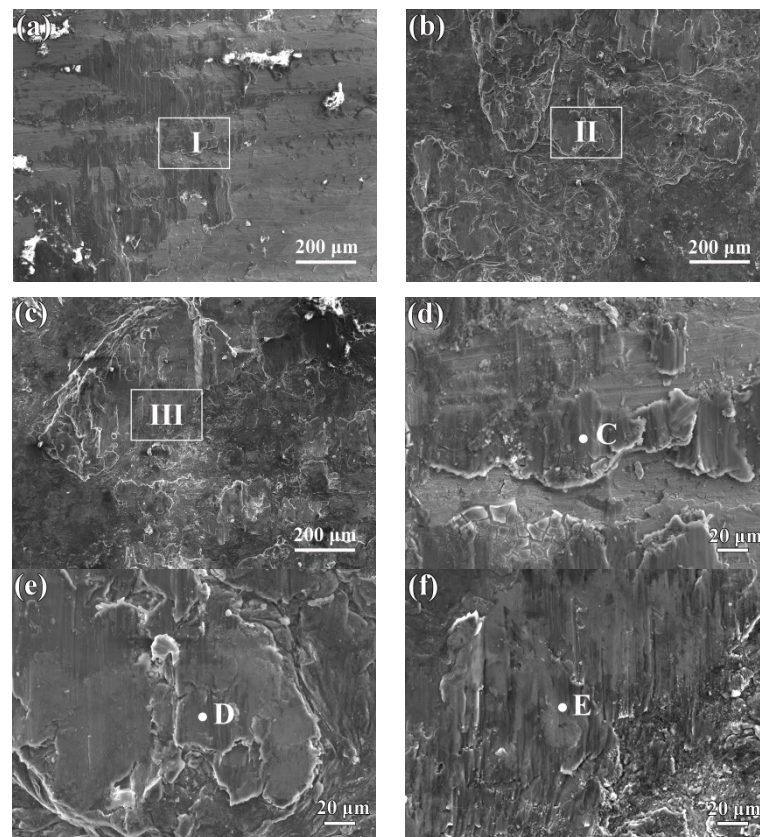

Figure 10. The load–displacement curves.

Figure 11. SEM fractographs on the Q235 side of the interface for the (**a**) AZ63/Q235, (**b**) AZ63/galvanized Q235, and (**c**) AZ63/galvanized Q235 + T6 push-out samples; (**d**–**f**) magnified image of the region I, II, and III, respectively.

Table 4. Shear strength of AZ63/Q235 metallurgical bonding with different heat treatment times.

Sample	Average Shear Strength (MPa)
AZ63/Q235	8.2 ± 0.4
AZ63/galvanized Q235	21.3 ± 0.5
AZ63/galvanized Q235 + T6	31.9 ± 1.9

Table 5. EDS results taken from points C, D, and E in Figure 11 (at.%).

Point	Mg	Al	Zn	Mn
C	94.2	4.9	0.7	0.2
D	94.4	2.6	2.6	0.4
E	96.2	2.6	1.1	0.1

The microhardness distributions across the interface of the AZ63/Q235, AZ63/galvanized Q235, and AZ63/galvanized Q235 + T6 are shown in Figure 12. The AZ63 matrix and Q235 matrix have average hardnesses of 70 and 210 HV, respectively. The average hardness of the AZ63 matrix increased to about 95 HV after T6 heat treatment. The hardness of the interface near the AZ63 matrix was significantly higher than that of the AZ63 matrix, and the interface of the AZ63/galvanized Q235 + T6 has the highest hardness, while the hardness of the AZ63/Q235 is the lowest. This is consistent with the change in shear strength. The hardness of Q235 near the interface is significantly lower than that of the Q235 matrix because the area is decarburized.
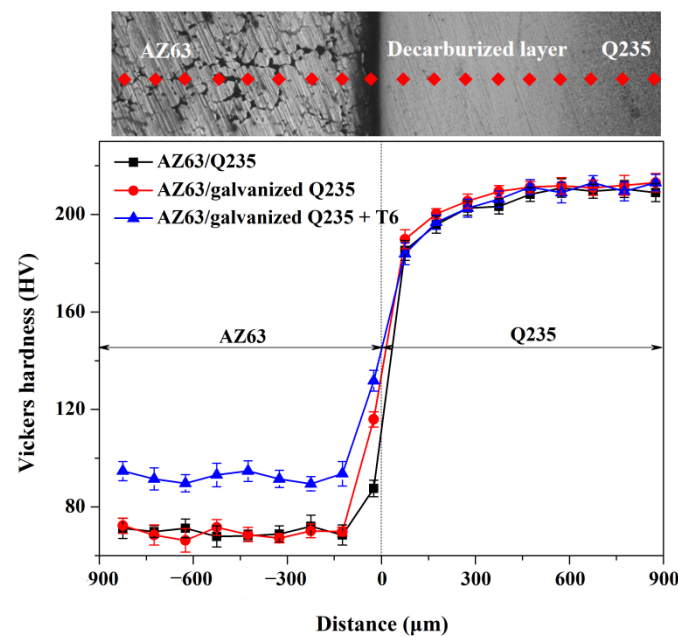
Figure 12. The microhardness distributions across the interface of the AZ63/Q235, AZ63/galvanized Q235, and AZ63/galvanized Q235 + T6.

4. Conclusions

The effects of Q235 hot-dip galvanized and post-casting T6 heat treatment on the interfacial reaction and mechanical properties of the AZ63/Q235 composite casting were investigated. The results can be summarized as follows:

1. The Q235 matrix of the AZ63/Q235, AZ63/galvanized Q235, and AZ63/galvanized Q235 + T6 treated samples formed a decarburized layer with a thickness of 300–350 μm near the interface. A small amount of intermetallic compounds was formed at the interface of AZ63/Q235, and a transition layer with an average thickness of about

15 μm was formed at the interface of AZ63/galvanized Q235. After T6 treatment, the average thickness of the interface transition layer between AZ63 and galvanized Q235 base layer was still about 15 μm, but the thickness of the transition layer became more uniform, and the size of the intermetallic compound was obviously refined.

2. The Al Mn, and Fe elements were obviously aggregated at the interface of AZ63/galvanized Q235. However, the zinc on the surface of the galvanized Q235 melted into the AZ63 magnesium alloy during the casting. After T6 treatment, the Al, Mn, and Zn elements in the matrixes were uniformly distributed, but the Al element at the interface was obviously increased, while the Mn element was obviously decreased. The intermetallic compound at the interfaces of AZ63/galvanized Q235 was $(Fe, Mn)_2Al_5$ before and after T6 treatment.

3. The shear strength of AZ63/Q235, AZ63/galvanized Q235, and AZ63/galvanized Q235 + T6 metallurgical bonding presents an increasing tendency. The hardness of the interface near the AZ63 matrix was significantly higher than that of the AZ63 matrix, and the interface of the AZ63/galvanized Q235 + T6 has the highest hardness, while the hardness of the AZ63/Q235 is the lowest.

Author Contributions: B.J., Q.Y. and J.Z. designed the project and guided the research; J.D. and Q.Z. performed the experiment and analyzed the data; Y.Z., Y.T., H.X. and C.P. investigated the project; J.D. wrote and reviewed the manuscript. All authors have read and agreed to the published version of the manuscript.

Institutional Review Board Statement: Not applicable.

Informed Consent Statement: Not applicable.

Data Availability Statement: Not applicable.

Conflicts of Interest: The authors declare no conflict of interest.

References

1. Parthiban, G.T.; Parthiban, T.; Ravi, R.; Saraswathy, V.; Palaniswamy, N.; Sivanb, V. Cathodic protection of steel in concrete using magnesium alloy anode. *Corros. Sci.* **2008**, *50*, 3329–3335. [CrossRef]

2. Kim, J.G.; Joo, J.H.; Koo, S.J. Development of high-driving potential and high-efficiency Mg-based sacrificial anodes for cathodic protection. *J. Mater. Sci. Lett.* **2000**, *19*, 477–479. [CrossRef]

3. Pathak, S.S.; Mendon, S.K.; Blanton, M.D.; Rawlins, J.W. Magnesium-based sacrificial anode cathodic protection coatings (Mg-rich primers) for aluminum alloys. *Metals* **2012**, *2*, 353–376. [CrossRef]

4. Yan, L.; Song, G.L.; Zheng, D. Magnesium alloy anode as a smart corrosivity detector and intelligent sacrificial anode protector for reinforced concrete. *Corros. Sci.* **2019**, *155*, 13–28. [CrossRef]

5. Li, J.; Chen, Z.; Jing, J.; Hou, J. Effect of yttrium modification on the corrosion behavior of AZ63 magnesium alloy in sodium chloride solution. *J. Magnes. Alloy.* **2021**, *9*, 613–626. [CrossRef]

6. Jafari, H.; Mohammad Hassanizadeh, B. Influence of Zr and Be on microstructure and electrochemical behavior of AZ63 anode. *Mater. Corros.* **2019**, *70*, 633–641. [CrossRef]

7. Kim, J.G.; Koo, S.J. Effect of alloying elements on electrochemical properties of magnesium-based sacrificial anodes. *Corrosion* **2000**, *56*, 380–388. [CrossRef]

8. Liu, L.; Qi, X.; Wu, Z. Microstructural characteristics of lap joint between magnesium alloy and mild steel with and without the addition of Sn element. *Mater. Lett.* **2010**, *64*, 89–92. [CrossRef]

9. Nayeb-Hashemi, A.A.; Clark, J.B.; Swartzendruber, L.J. The Fe-Mg (Iron-Magnesium) system. *Bull. Alloy. Phase Diagr.* **1985**, *6*, 235–238. [CrossRef]

10. Patel, V.K.; Bhole, S.D.; Chen, D.L. Formation of zinc interlayer texture during dissimilar ultrasonic spot welding of magnesium and high strength low alloy steel. *Mater. Des.* **2013**, *45*, 236–240. [CrossRef]

11. Sacerdote-Peronnet, M.; Guiot, E.; Bosselet, F.; Dezellus, O.; Rouby, D.; Viala, J.C. Local reinforcement of magnesium base castings with mild steel inserts. *Mat. Sci. Eng. A* **2007**, *445*, 296–301. [CrossRef]

12. Cheng, J.; Zhao, J.; Zhang, J.; Guo, Y.; He, K.; Shang-Guan, J.; Wen, F. Microstructure and mechanical properties of galvanized-45 steel/AZ91D bimetallic material by liquid-solid compound casting. *Materials* **2019**, *12*, 1651. [CrossRef]

13. Cheng, J.; Zhao, J.; Zheng, D.; He, K.; Guo, Y. Effect of the vacuum heat treatment on the microstructure and mechanical properties of the galvanized-Q235/AZ91D bimetal material produced by solid-liquid compound casting. *Met. Mater. Int.* **2021**, *27*, 545–555. [CrossRef]

14. Jiang, W.; Jiang, H.; Li, G.; Guan, F.; Zhu, J.; Fan, Z. Microstructure, mechanical properties and fracture behavior of magnesium/steel bimetal using compound casting assisted with hot-dip aluminizing. *Met. Mater. Int.* **2021**, *27*, 2977–2988. [CrossRef]

15. Zhao, J.; Zhao, W.; Shen, Q.U.; Zhang, Y.Q. Microstructures and mechanical properties of AZ91D/0Cr19Ni9 bimetal composite prepared by liquid-solid compound casting. *Trans. Nonferrous Met. Soc. China* **2019**, *29*, 51–58. [CrossRef]

16. Kartsonakis, I.A.; Stanciu, S.G.; Matei, A.A.; Hristu, R.; Karantonis, A.; Charitidis, C.A. A comparative study of corrosion inhibitors on hot-dip galvanized steel. *Corros. Sci.* **2016**, *112*, 289–307. [CrossRef]

17. Chen, Y.C.; Nakata, K. Friction stir lap welding of magnesium alloy and zinc-coated steel. *Mater. Trans.* **2009**, *50*, 2598–2603. [CrossRef]

18. Jafari, H.; Idris, M.H.; Ourdjini, A.; Payganeh, G. Effect of thermomechanical treatment on microstructure and hardness behavior of AZ63 magnesium alloy. *Acta Metall. Sin.* **2009**, *22*, 401–407. [CrossRef]

19. Takeuchi, A.; Inoue, A. Classification of bulk metallic glasses by atomic size difference, heat of mixing and period of constituent elements and its application to characterization of the main alloying element. *Mater. Trans.* **2005**, *46*, 2817–2829. [CrossRef]

20. Li, X.; Scherf, A.; Heilmaier, M.; Stein, F. The Al-rich part of the Fe-Al phase diagram. *J. Phase. Equilib. Diff.* **2016**, *37*, 162–173. [CrossRef]

21. Shi, Y.; He, C.C.; Huang, J.K.; Fan, D. Thermodnamic Analysis of the Forming of Intermetallic Compounds on Aluminium-Steel Welding Interface. *J. Lanzhou Univ. Technol.* **2013**, *39*, 45–47.